Journal of Mines, Metals and Fuels, 70(8) : 440-448; 2022. DOI: 10.18311/jmmf/2022/32528

Print ISSN : 0022-2755

Journal of Mines, Metals and Fuels

Contents available at: www.informaticsjournals.com/index.php/jmmf

Characteristics of Various Losses of Axial Piston Pump and Bent Axis Hydro-motor with respect to Displacement Conditions and Load Demands

Ajit Kumar Pandey[1], Amit Kumar[1] and Ajit Kumar[2*]

[1]Department of Mechanical Engineering, National Institute of Technology, Patna – 800005, Bihar, India
[2]Department of Mechanical Engineering, Indian Institute of Technology (Indian School of Mines), Dhanbad, Jharkhand – 826004, India; ajit@iitism.ac.in

Abstract

The hydrostatic transmission is one of the most important applications in the fluid power systems. It gives smooth change in output speed, torque and power as per the design requirements. Present article deals with various losses of the hydraulic pump and motor using a closed circuit hydraulic drive. The drive basically consists of a variable displacement axial piston pump that supplies pressurized fluid to a variable displacement bent axis hydro-motor. In investigating the pump/motor performance, bond graph simulation technique is used to model the drive system. Various losses of the pump and motor are accounted in the model by suitable resistive elements. The characteristics of them are identified through experiments. The predicted performance of the pump/motor is studied with respect to the displacement and load at the same time they are validated experimentally. The investigation made in the article identifies the control strategy which will be useful for the practicing engineers to select best combination of the pump and motor displacement for optimizing the drive performance and minimizing the losses as well. The study performed in this research work will be useful for the similar hydraulic configuration used in mobile equipment.

Keywords: *Axial Piston Pump, Bond Graph Modelling, Displacement Ratio, Hydrostatic Drive (HST), Hydro-motor*

1.0 Introduction

HST drives are used in heavy mobile machinery for its high-power density, wider speed-torque range and good efficiency. While analyzing the performance of such drive, it is important to consider its various losses.

Most of the models of the pumps and hydro-motors currently being used are based on the losses proposed by notable researchers (Wilson WE, (1949); Schlösser, W (1961); Zarotti G and Nervegna, (1981); Hydrostatic Pumps and Motors (1993); Conrad F, *et al.* (1993); Mandal SK, *et al.* (2009); Kumar and Dasgupta, (2015); Williamson and Ivantysynova, (2007); Rahmfeld and Eckhard, (2010); Lux and Murrenhoff, (2016); Hasan, *et al.*, (2015); Kohmäscher *et al.*, (2007)). However, investigating various losses of the variable displacement pump and the variable displacement motor in HST drive is presented in this article which has not yet been studied.

Understanding the losses of the hydrostatic drive, rather pragmatic approach is followed due to the complicated flow mechanics involved in the components.

*Author for correspondence

This article characterizes the different losses of the hydraulic pump/motor using a closed circuit hydraulic drive, where both the pump and the motor are variable. By adjusting the displacements of the pump, the losses have been investigated for wide torque–speed range.

The studies conducted will be useful to develop its design guidelines from where the components of the HST drive could be selected without developing a prototype to get test data.

In analyzing the pump and motor losses, mathematical models of the pump and the motor are made, where the pump and the motor losses are considered by suitable resistances. Chamber volume variation of a multi-piston pump or the motor with respect to its shaft rotation along with their losses demands a structured approach to develop its mathematical model (Dasgupta, and Mondal, (2002)). The Bond graph gives such an approach in a simplified way (Thoma, (1990)). A steady-state model of the drive is developed, where various resistances represent the pump and the motor losses. The non-linear characteristics of the losses that depend upon various state-variables of the system are identified through test results. Compared with the experimental results, the model is validated. Using the validated model, various losses of the hydraulic components is studied. The model presented in this article guides the design of the experiment and mode of data handling of the observations in such a way that the dependency of the parameters on the operating conditions of the pump and the motor of the HST drives are obtained. The model is found to be highly adaptable and it agrees fairly well to the experimental data. This enhances the reusability of the model and improves its predictivepower.

2.0 Physical System

From Figure 1, where a variable displacement pumps driven by a constant speed prime mover supplies flow to a hydro-motor. The load on the hydro-motor shaft is provided by suitable loading unit, whereby controlling the pump and the valve, the load on the motor is varied.

Figure 2 shows the variable displacement bent axis hydro-motor (Product literature of the variable displacement bent axis hydro-motor, Bosch Rexroth (I) Ltd.) considered in the studies, where the pump supplies pressurized fluid to its seven pistons, which reciprocate inside the cylinder block. With the movement of the pistons, the hydro-motor rotates. By varying the angle between the axis of the drive shaft and the cylinder block, the speed and the torque of the drive are controlled.

Figure 3 shows the variable displacement axial piston pump (Product literature of the variable displacement in-line pump, Bosch Rexroth (I) Ltd.), where due to rotation of the cylinder block, pistons inside it reciprocate. By varying the swash plate angle (α), piston stroke changes and so does the pump flow.

For the analysis of the pump and the motor, various leakage passages are shown in Figures 2 and 3. Leakage flow paths are as follows:

a) Leakage flow through the annular region (Q_{al}).
b) Leakage flow through clearances between the ball and socket joint (Q_s).

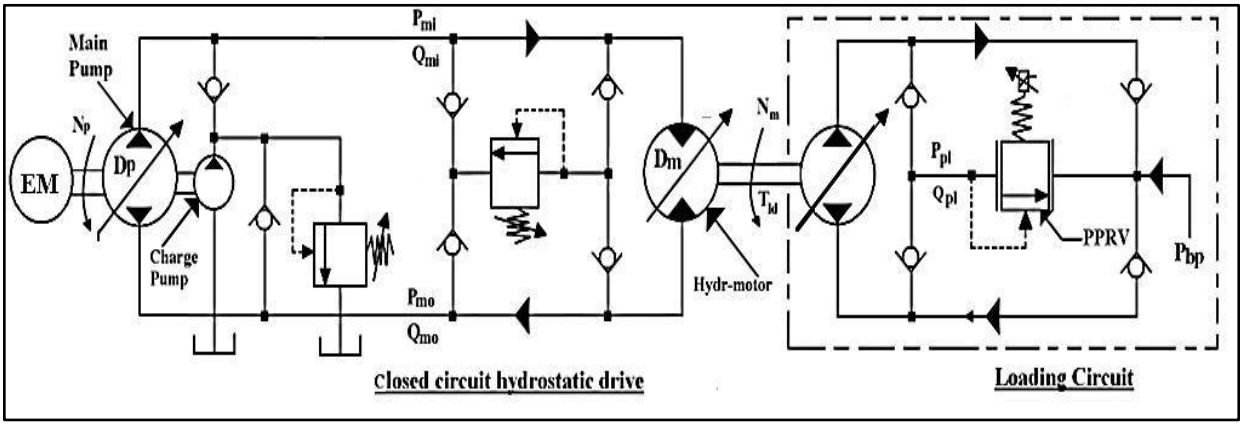

Figure 1. Closed circuit hydrostatic drive with variable pump and motor.

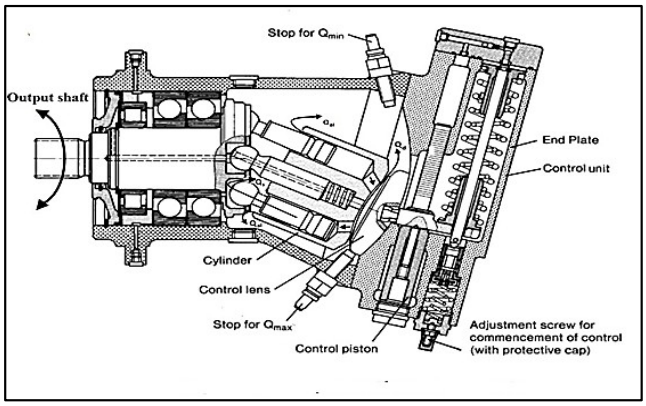

Figure 2. Bent axis hydro-motor (Variable displacement volume).

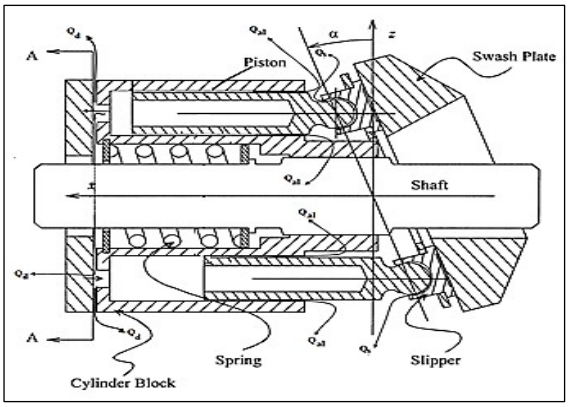

Figure 3. Axial piston pump (Variable displacement volume). The detailed overview of the pump as well as the motor is provided in the textbook (Watton (2009)).

Table 1. List of components used in the test set-up.

sr. no.	Items	Model/ Make
1	Variable displacement axial piston pump maximum displacement 28 cc/rev	Model-A4VG28EP2DM1/3X–RPZC10F02D Bosch Rexroth, Germany
2	Variable displacement Bent-axis hydro-motor Maximum displacement 28 cc/rev	Model- A2FM16/61W-VBB030 Bosch Rexroth, Germany
3	Torque sensor Accuracy-1% of full scale torque Max. torque range- 100 Nm	Model-K-T40B-100Q-MF-S-M-DU2-0-S HBM, Germany
4	Flow sensor Turbine type flow sensor accuracy ±0.5% Flow range- 0-60 LPM	Model- TFM 1015 Rockwin Flow meter India Pvt. Ltd
5	Speed sensor Non-contact type Accuracy ±1 RPM or 0.005% of reading optical speed range- (0-2500 rpm)	Model - ROS-W Monarc Instrument, USA.
6	Pressure sensor Accuracy - 0.25 % pressure range - (0-200 bar)	Model- S10 Wika, Germany

c) Leakage flow through clearances through the valve plate and cylindrical barrel (Q_d). Taking together the above leakages, it is considered as external leakage in the model.

Similarly, internal leakage of the pump (Q_{ilp}) and the motor (Q_{ilm}) are also considered in the model.

The detailed of the experimental set-up and its working is given in Appendix 1

3.0 Modeling of the System

While developing the steady-state model of the system:

- The leakage flow in the model other than above discussed for the pump and the motor is not taken into account.
- The effects of the resistance and the capacitance of the hydraulic fluid flow passage are lumped, wherever appropriate.
- The temperature and pressure effects on fluid properties are not considered.
- The hydraulic oil used in the experiment is a Newtonian fluid.
- The line resistance is not taken into account in the present study.

The Bond graph model of the system is shown in Figure 4. A hydraulic displacement machine translates

hydraulic power to mechanical power or vice-versa. The displacement ratios of the pump (β_{pd}) and the hydro-motor (β_{md}) are represented by the modulated transformer (*TF*) junctions. Being bilateral in nature, the TFs also convert pressure of the chamber to the shaft torque.

The SF element in Figure 4, with 1 junction shows the speed (Np) of the pump. The pressure drop across the *p* valve ports of the pump arises due to fluid flow through it. Combining this with the frictional loss, the total mechanical loss of the pump is represented by the resistive element R_{pd} attached with 1_{Np} junction. The leakage flow of the pump represented by the resistance R_{pl} appear as R element on the pump plenum, 0_{pp} junction. The C element on the same junction indicates the bulk stiffness of the hydraulic fluid K_{cp} at the pump plenum. The pump supplies flow V_p to the inlet port (R_{vm}) of the motor, from where it moves to the motor plenum, as represented by 0_{pm} junction. Like the pump, R_{ml} of the motor represents its leakage resistance. The motor converts the hydraulic power to the mechanical power that drives the load. The SE element on 1_{Nm} junction represents the torque load. Such element determines the differential pressure across the motor. The C element attached to the same junction observes the motor speed.

The transformer moduli V_p and V_m indicates the pump and the motor volumetric displacement. The expression for displacement rates of the hydraulic units (pump and hydro-motor) are given by:

$$Vp = \beta_{pd} Vp_{\max}$$

$$\text{and } Vm = \beta_{md} Vm_{\max}$$

where, $V_{p\max}$ and $V_{m\max}$ are the maximum displacement rate of the pump and the motor, respectively.

The torque loss of the HST drive mainly depends on the resistance R_{pd} and R_{vm}.

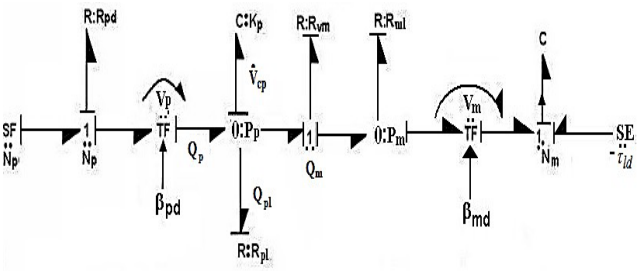

Figure 4. Reduced model of the HST drive.

Similarly, leakage resistances R_{ml} and R_{pl} take into account the volumetric efficiency of the drive. Their characteristics are collected from the test outcomes given in Section 4.

The expressions deduced from the model are as follows: Flow loss due to fluid compressibility is given by:

$$\dot{V}_{cp} = N_p \beta_{pd} \left(V_{p\max} - \frac{P_p}{R_{pl}} - \frac{(P_p - \frac{\tau_{ld}}{V_m})}{R_{vm}} \right) \quad (1)$$

In the above expression, the 2nd term represents the ideal discharge of the pump, whereas; the 3rd and the 4th term indicate the leakage of the pump and motor inlet flow, respectively.

Ignoring the fluid compressibility loss in Eq. (1), the above expression reduced to

$$R_{vm} = \frac{P_p}{N_p V_p - \frac{P_p}{R_{pl}} - \frac{\tau_{ld}}{V_m}} \quad (2)$$

The leakage flow of the pump is given as:

$$Q_{pl} = \frac{P_p}{R_{pl}} \quad (3)$$

Leakage flow of the hydro-motor is expressed as:

$$Q_{ml} = \frac{\tau_{ld}}{V_m R_{pl}} \quad (4)$$

The Pump torque is given by:

$$\tau_{ld} = P_p V_p + R_{pd} N_p \quad (5)$$

The pump drag resistance is given by:

$$R_{pd} = (\beta_p - P_p V_p) / N_p \quad (6)$$

4.0 Comparison of Model with Experimental Outcome and Discussion

The main objective of the test programme is to validate the model proposed in the article with the test data. In this

respect, the overall efficiency of the system was examined with respect to the pump and the motor displacement ratios at different torque-level. At the onset, the characteristics of the losses were found experimentally.

4.1 Validation of the Pump and the Hydro-motor Losses

At different load torque, the losses were determined for the pump and the motor with respect to their displacements (V_p) and (V_m), respectively. Substituting the test data of the pump torque (τ_p), pump speed (N_p), load torque (ld), maximum displacements of the pump and the hydro-motor in Eqs. (2) through (5), the nature of the loss characteristics are identified. The test data were collected for the torque and the speed range of 28-50 Nm and of 400–2600 r_{pm}, respectively, where maximum system pressure was 120 bar. Due to limitation of the test set up, the displacement of the pump and the hydro-motor (V_m) could not be lowered below 40% of its maximum value. Accordingly, the characteristics of the losses were obtained and they are provided in Appendix 1.

From the Figures 5 and 9, it is found that with increasing pump displacement ratio (β_{pd}) or the motor displacement ratio (β_{md}), leakage resistance of the pump (R_{pl}) increases. Leakage resistance (R_{ml}) of the hydro-motor decreases with increase in the displacement ratio of the pump (β_{pd}), whereas Rml increases with the increase in the displacement ratio of the motor (β_{md}) as indicated in Figures 6 and 10.

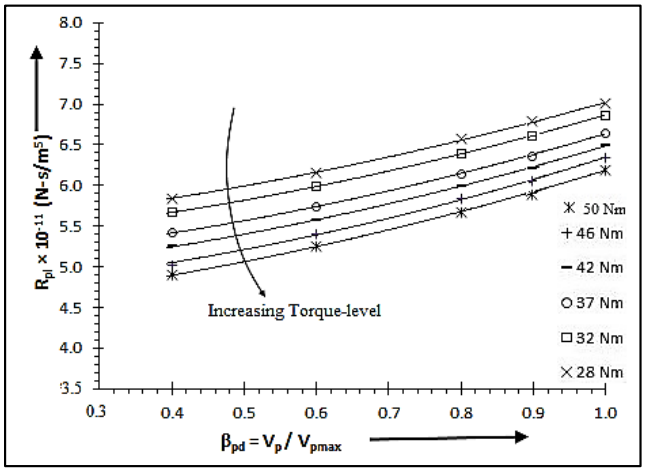

Figure 5. Characteristic of the leakage resistance (R_{pl}) of the pump in HST drive with respect to the varying pump displacement.

Figures 7 and 11 indicate the characteristics of the motor valve port resistance (R_{vm}) that translates into the torque loss of the drive. It is noticed that with the rise in the displacement ratio of the pump (β_{pd}), such resistance (R_{vm}) decreases; whereas by increasing the displacement ratio of the motor (β_{md}), R_{vm} increases. An increase in the load-torque (ld) for a constant displacement ratio of the pump (β_{pd}), valve port resistance (R_{vm}) decreases; thereby torque losses of the drive also reduces shown in Figure 7, which leads to higher mechanical efficiency. Such efficiency of the drive decreases, with the rise in the torque for a constant displacement ratio of motor (β_{md}) as shown in Figure 11.

From the Figures 8 and 12, it is found that characteristic of the pump drag resistance (R_{pd}) rises with the rise in the pump displacement ratio (β_{pd}), whereas, it decreases with the increase in the displacement ratio of the hydro-motor (β_{md}) for the same load torque. The drag resistance R_{pd} increases with the increase in the load torque at a fixed displacement ratios of the pump (β_{pd}) and the hydro-motor (β_{md}). Like the hydro-motor, the mechanical efficiency of the pump is affected by drag resistance.

Using the test data in Eq. (2) for different torque level, the predicted characteristics of R_{vm} are compared in Figures 13 and 14. It is found that the predicted and the experimental results are very close to each other, differ by ± 1% to ± 2%, which seems to be reasonable. In the same way, the polynomial expressions of other loss-coefficients (R_{pl}, R_{ml}, and R_{pd}) could be established by further examination.

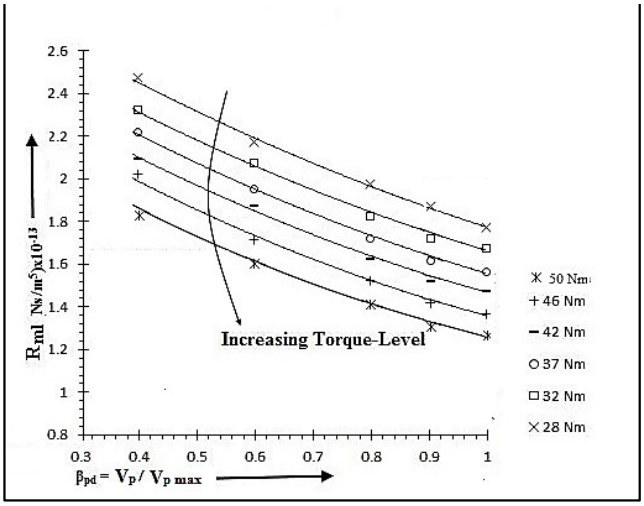

Figure 6. Characteristic of the leakage resistance (R_{ml}) of the motor in HST drive with respect to the varying pump displacement.

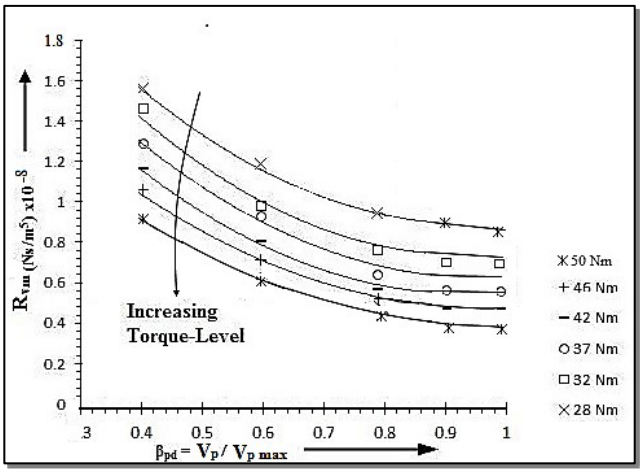

Figure 7 Characteristic of the valve port resistance (R_{vm}) of the motor in HST drive with respect to the varying pump displacement.

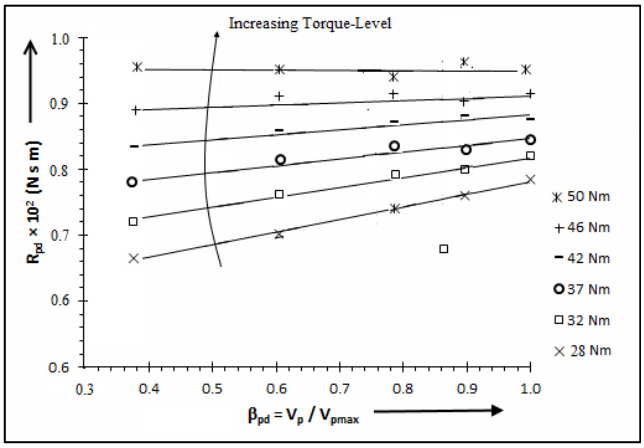

Figure 8. Characteristic of the drag resistance (R_{pd}) of the pump in HST drive with respect to the varying pump displacement.

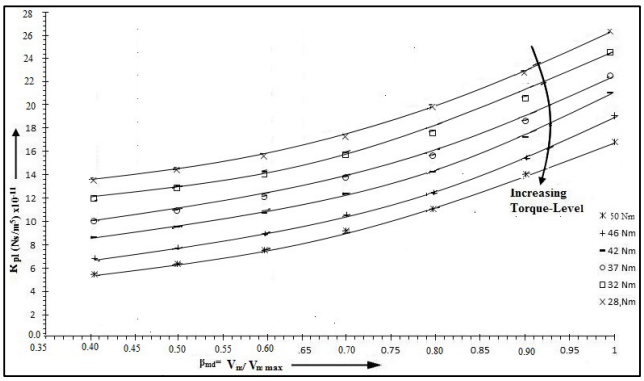

Figure 9. Characteristic of the leakage resistance (R_{pl}) of the pump in HST drive with respect to the varying motor displacement.

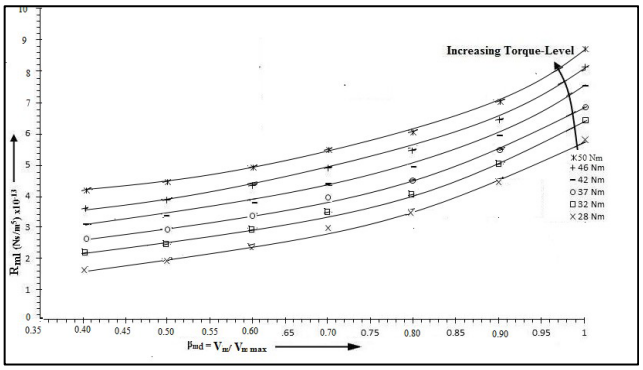

Figure 10. Characteristic of the leakage resistance (R_{ml}) of the motor in HST drive with respect to the varying motor displacement.

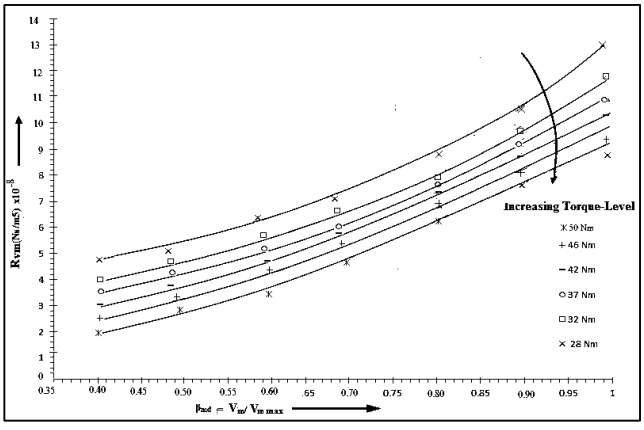

Figure 11. Characteristic of the valve port resistance (R_{vm}) of the motor in HST drive with respect to the varying motor displacement.

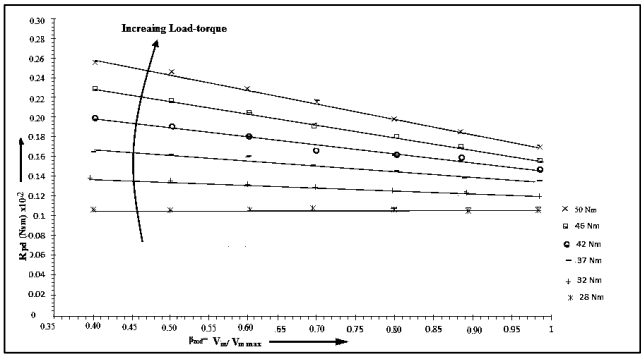

Figure 12. Characteristic of the drag resistance (R_{pd}) of the pump in HST drive with respect to the varying motor displacement.

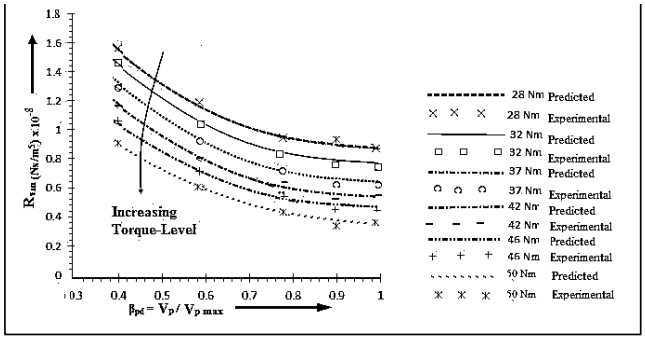

Figure 13. Comparison of the predicted and the experimental nature of valve port resistance R_{vm} of the motor in HST drive with respect to the varying motor displacement.

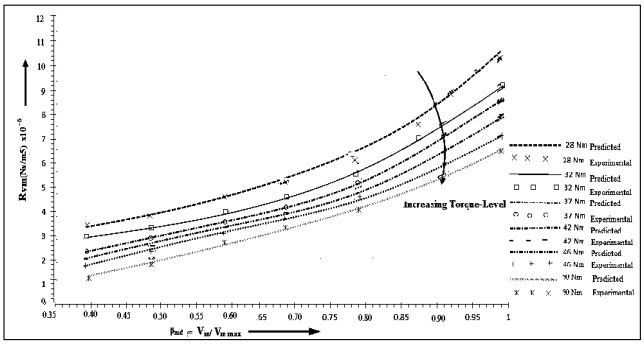

Figure 14. Comparison of the experimental and the predicted nature of valve port resistance R_{vm} of the motor in HST drive with respect to the varying motor displacement.

Similar trend of the resistances given were found by McCandlish (1984) and Mandal *et al.* (2009) in their studies on the plunger type hydro-static unit. The variation of R_{vm} described by the quadratic relationship was also observed by Thoma (1969) and Schösser (1961).

5.0 Conclusions

In this article, various losses of the pump and motor in a closed circuit HST drive have been studied with respect to the variation in the displacement of the pump and the hydro-motor. In this respect, bond graph simulation technique is used in modeling the HST drive. A reduced bond graph model is proposed, where various losses are taken into account by suitable resistive elements. Such a model has fewer parameters and needs reduced number of test-runs to establish them. The loss coefficients of the drive indicate that they vary with the load torque and displacement of the pump and the hydro-motor, a behaviour that was also recognized by Mandal *et al.* (2009) and Kumar *et al.* (2015). The losses found to have a non-linear relationship with the load torque and displacement rate of the pump and the hydro-motor. Using them, the performance parameters of the drive such as the slip, torque loss and efficiency could be established. From the study, suitable control strategy can be established for the maximum operating efficiency of the hydraulic components.

The conclusions drawn from the study are as follows:

- With the variation of the pump and the motor displacements, the pump leakage resistance (R_{pl}) decreases with an increase in the load torque (*ld*) as shown in Figures 5 and 9.
- The hydro-motor leakage resistance (R_{ml}) reduces with the rise in the displacement of the pump, whereas, with an increase in the motor displacement, such resistance increases. At a given speed (ω_m), R_{ml} rises with the rise in torque level as shown in Figures 6 and 10.
- The valve port resistance of the motor (R_{vm}) reduces with increase in the displacement of the pump, whereas, it (R_{vm}) increases with increase in displacement of the motor. For a constant drive speed, R_{vm} decreases with increase in load torque as shown in Figures 7 and 11. The pump drag resistance (R_{pd}) rises with rise in βpd, whereas, it (R_{pd}) reduces with decreasing β_{md} as presented in Figures 8 and 12.

Losses of the hydraulic components discussed in this article do not represent the performance of all hydraulic pump and motor, as it will differ among the manufacturers. Further refinement of the model is feasible if the ignored minor losses due to thermal effects, hydrodynamic losses etc., are considered, that needs more detailed theoretical analysis and rigorous experiments.

By measuring slip and torque losses a suitable control schemes may be formulated for varying displacement ratios of the pump and motor to optimize the performance of the hydraulic components. This may be a potential future work

The reduced model proposed in this article may be useful to the practicing engineers in the selection of similar HST drives. It may be also helpful to analyze the control aspects of the plant, where proposed drive is an integral part

6.0 References

1. Wilson, W. E. (1949). Performance criteria for positive displacement pumps and fluid motors. *Transactions of the American Society of Mechanical Engineers*, *71*(2), 115–20.
2. Schlösser, W. (1961). Mathematical model for displacement pumps and motors. *Hydraulic Power Transmission,* 324–328.
3. Zarotti, G., & Nervegna, N. (1981). Pump efficiencies approximation and modelling. 145–164.
4. Hydrostatic Pumps and Motors. (1993). Design and calculation.
5. Conrad F., Trostmann E., & Zhang M. (1993). Automatic computer controlled bi-directional dynamometer applied for identification of static performance and experimental modelling of losses in hydraulic pumps and motors, 3rd SICFP. Linköping, Sweden.
6. Mandal, S. K., Dasgupta, K., Pan, S., Chattopadhyay, A. (2009). Theoretical and experimental studies on the steady-state performance of low-speed high-torque hydrostatic drives. Part 2: Experimental investigation. *Proceedings of the Institution of Mechanical Engineers, Part C: Journal of Mechanical Engineering Science*. *223*(11), 2675–85. https://doi.org/10.1243/09544062JMES1203
7. Kumar, N., & Dasgupta, K. (2015). Steady-state performance investigation of hydrostatic summation drive using bent-axis hydraulic motor. *Proceedings of the Institution of Mechanical Engineers, Part C: Journal of Mechanical Engineering Science, 229*(17), 3234–51. https://doi.org/10.1177/0954406214559410
8. Williamson, C., & Ivantysynova, M. (2007). The effect of pump efficiency on displacement-controlled actuator systems. *Proceedings of the Tenth Scandinavian International Conference on Fluid Power, Tampere, Finland, 2,* 301–326.
9. Rahmfeld, R., & Eckhard. (2010). Efficiency measurement and modelling - essential for optimising hydrostatic systems. *7th International Fluid Power Conference,* 1–14, Aachen.
10. Lux, J., & Murrenhoff, H. (2016). Experimental loss analysis of displacement controlled pumps. *10th International Fluid Power Conference,* 441–451, Dresden.
11. Hasan, M. E., Dasgupta, K., & Ghoshal, S. (2015). Comparison of the efficiency of the high speed low torque hydrostatic drives using bent axis motor: An experimental study. *Proceedings of the Institution of Mechanical Engineers, Part E: Journal of Process Mechanical Engineering*, 11. https://doi.org/10.1177/0954408915622413
12. Kohmäscher, T., Rahmfeld, R., Murrenhoff, H., & Skirde, E. (2007). Improved loss modeling of hydrostatic units: requirement for precise simulation of mobile working machine drivelines. *International Mechanical Engineering Congress and Exposition. American Society of Mechanical Engineers,* 195–206. https://doi.org/10.1115/IMECE2007-41803
13. Dasgupta, K., Mondal, S. K. (2002). Analysis of the steady-state performance of a multi-plunger hydraulic pump. *Proceedings of the Institution of Mechanical Engineers, Part A: Journal of Power and Energy,* 216(6), 471–419. https://doi.org/10.1243/095765002761034249
14. Thoma, J. U. (1990). Simulation by bondgraph. Springer, Berlin. https://doi.org/10.1007/978-3-642-83922-1
15. Product literature of the variable displacement bent axis hydro-motor, Bosch Rexroth (I) Ltd.
16. Product literature of the variable displacement in-line pump, Bosch Rexroth (I) Ltd.
17. Watton, J. (2009). Fundamentals of fluid power control. Cambridge University Press, *10*. https://doi.org/10.1017/CBO9781139175241
18. McCandlish, D., & Dorey, R. E. (1984). The mathematical modelling of hydrostatic pumps and motors *Proceedings of the Institution of Mechanical Engineers, Part B: Management and Engineering Manufacture*. *198*(3), 165–74. https://doi.org/10.1243/PIME_PROC_1984_198_062_02
19. Mandal, S. K., Dasgupta, K., Pan, S., & Chattopadhyay. (2009). A Theoretical and experimental studies on the steady-state performance of low-speed high-torque hydrostatic drives. Part 1: modelling. *Proceedings of the Institution of Mechanical Engineers, Part C: Journal of Mechanical Engineering Science*, *223*(11), 2663–2674. https://doi.org/10.1243/09544062JMES1202
20. Thoma, J. U. (1969). Mathematical models and effective performance of hydrostatic machines and transmission. *Hydraul Pneumatic Power,* 642–651.
21. BS 4617. (1983). Methods of testing hydraulic piston pumps and motors for hydrostatic power transmission. British Standards Institution, London.

Appendix

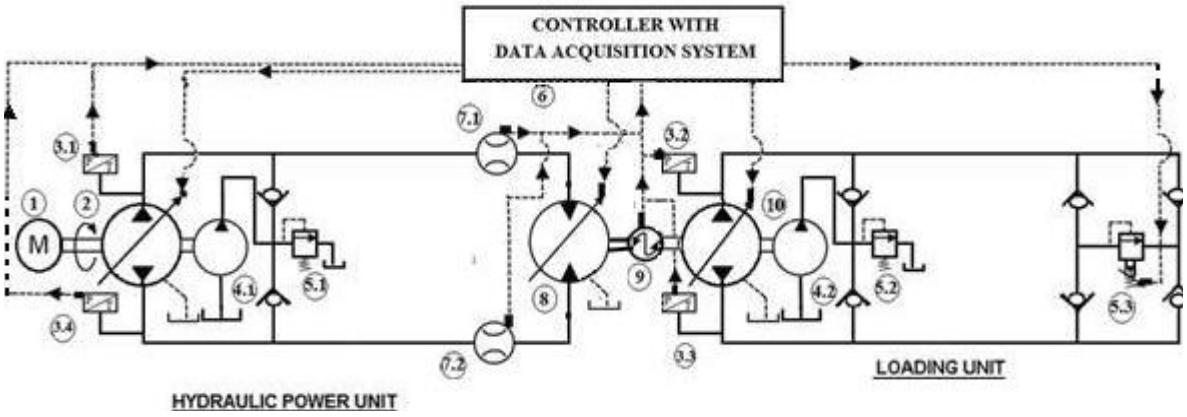

Figure 15. Schematic diagram of the experimental test-up

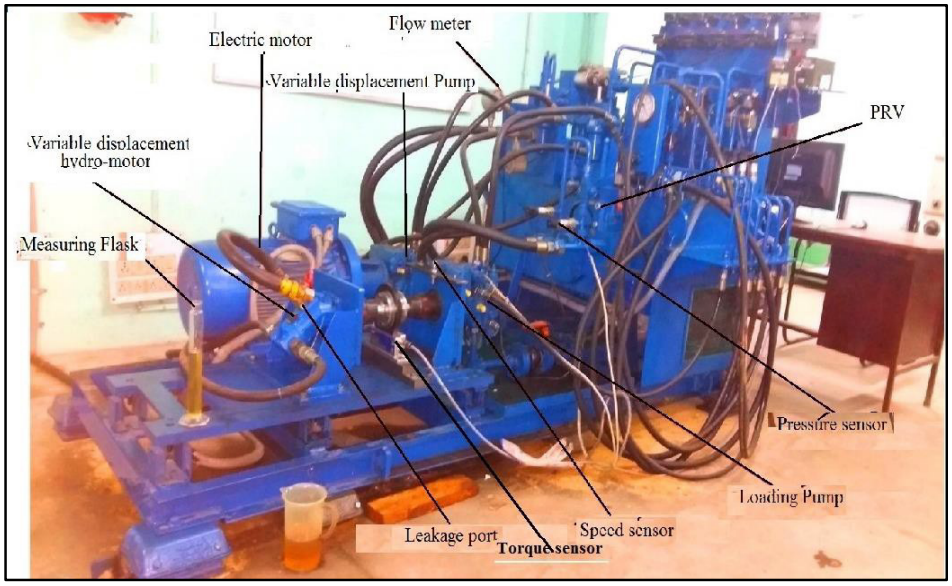

Figure 16. Pictorial view of the test rig of the closed circuit HST drives

In the test set-up, a variable displacement pump driven by an electric motor at a constant speed supplies pressurized fluid to the hydro-motor; that, in turn, drives a pump of loading circuit. By controlling the displacement of the pump or the motor as well as adjusting the pressure of the relief valve in the loading circuit, the torque load of the hydro-motor is varied. The torque and speed of the hydro-motor and also the pressure and flow of the pump are stored in the data acquisition system The displacement of the pump and the motor are adjusted from the control panel for a targeted torque and speed of the drive. During experiment, the fluid temperature was maintained within 50±20C. The pressure difference across the hydraulic machine was kept constant with reasonable accuracy during the experiment.

By using the pressure, flow, torque and speed sensors, the test data were collected and before conducting experiments all of them were calibrated. The experiments were conducted for the drive speed that ranges from 400 rpm to 2600 rpm; whereas, load torque and operating pressure was varied from 28 Nm to 50 Nm and 63-120 bar, respectively. The experiments could not be performed for higher torque range due to limitations of the set-up. Repeated test runs were made following a standard test procedure (BS 4617, (1983)).